Solid State Communications 150 (2010) 564–567

Contents lists available at ScienceDirect

Solid State Communications

journal homepage: www.elsevier.com/locate/ssc

The magnetoelastic effect in $Co_xMn_{1-x}S$ solid solutions

S.S. Aplesnin [a,*], L.I. Ryabinkina [a], O.B. Romanova [a], A.M. Har'kov [a], M.V. Gorev [b], A.D. Balaev [b], E.V. Eremin [b], A.F. Bovina [b]

[a] M.F. Reshetneva Aircosmic Siberian State University, Krasnoyarsk, 660014, Russia

[b] Center of shared using KSC Siberian branch of Russian Academy Science, Krasnoyarsk, 660036, Russia

article info

Article history:
Received 14 November 2009
Accepted 8 January 2010
by E.L. Ivchenko
Available online 15 January 2010

Keywords:
A. Semiconductors
C. X-ray scattering
D. Galvanomagnetic effects
D. Thermal expansion

abstract

The magnetization of cation-substituted $Co_xMn_{1-x}S$ sulfides upon cooling in zero magnetic field and in a field in the temperature range 4–300 K has been measured and the resistance versus magnetic field (up to 10 kOe) dependences have been obtained. Magnetoresistance and temperature hysteresis of magnetization versus prehistory are found at the magnetic field $H < 0.1$ T and at $T < 240$ K. The interrelation between the magnetic and elastic subsystems of the $Co_xMn_{1-x}S$ solid solutions has been established. A jump in the coefficient of thermal expansion is observed at the Néel temperature. The features of the physical properties are explained by orbital ordering.

1. Introduction

An active role of the orbital degree of freedom in the lattice [1] and an electronic response can be most typically seen in manganese oxide compounds with the perovskite structure [2–4]. But the orbital physics are universal in transition-metal oxides. For the classic material V_2O_3, which has the corundum structure, two electrons occupy t_{2g} orbitals. In the conventional view, the orbital ordering in the E_g state of the original t_{2g} manifold has been assigned to the origin of the specific spin order in the AF ground state [5]. An effective Hamiltonian for the spin and the orbital has been derived on the basis of this picture, and the magnetic properties have been discussed. The important feature is that the magnetic exchange interaction depends on the orbital occupancy; i.e., even the sign could change [6]. Therefore, it is possible that the magnetic correlation in the normal state can be very different from that in the ordered phase when the orbital order is accompanied by a magnetic transition, as observed experimentally.

A more transparent example is the case of perovskite-type $RTiO_3$ [7] and RVO_3 [8,9] with $3d_1$ and $3d_2$ electron configuration, respectively, both retaining the orbital degree of freedom in the t_{2g} state. The actual orbital order pattern in these t_{2g} electron systems is not straightforwardly visible from the crystal structure alone because of the relatively weak Jahn–Teller (JT) distortion of the t_{2g} electron. This is in contrast to the case of an e_g electron with strong JT distortion. An example of dynamical orbital correlation is seen in the spin-state transition in $LaCoO_3$ with $3d_6$ configuration of Co [10]. In fact, the correlated local lattice distortion clearly shows up in the infrared phonon spectra in accord with the spin-state crossover [11], although the average lattice structure appears to be undistorted from that of the ground state. This is another example of a thermally induced dynamical JT effect due to short-range orbital order. However, $LaCoO_3$ undergoes the insulator-to-metal transition on warming above 500 K. As predicted by the local density approximation (LDA) calculation [10], this phenomenon may be interpreted as the loss of the orbital (short-range) order. Therefore, the orbital correlation and the spin correlation are expected to play an important role in magnetoelastic interactions.

Promising materials are $Co_xMn_{1-x}S$ solid solutions, which assume orbital ordering [12,13]. Due to the different electronegativities of the cobalt and manganese ions, the electron density at the t_2g shell of Mn ions in solid solution can be higher than in MnS. To qualitatively consider the magnetic and electric properties, we will restrict ourselves to a simple primitive model describing the interaction of an electron on the Co ions having only Mn ions in their nearest environment. The interaction with phonons may lead to the distortion of octahedra along one of the axes that are degenerate in a face-centred cubic (FCC) lattice. This degeneracy will determine the spin-glass properties, which manifest themselves in external magnetic and electric fields. The purpose of this study is to establish the relationship between the magnetic and elastic subsystems.

2. Experimental results

The crystal structure of the $Co_xMn_{1-x}S$ sulfides was studied at 300 K in monochromatic Cu K radiation with a DRON-3 facility.

* Corresponding author.
E-mail address: apl@iph.krasn.ru (S.S. Aplesnin).

0038-1098/$ – see front matter © 2010 Elsevier Ltd. All rights reserved.
doi:10.1016/j.ssc.2010.01.009

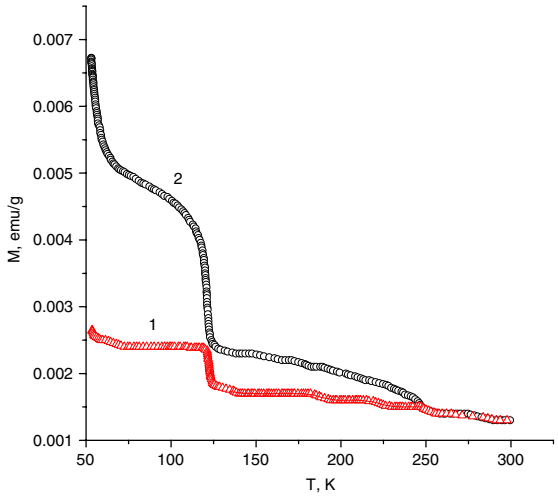

Fig. 1. Temperature dependences of magnetization upon cooling in a magnetic field $H = 100$ Oe (curve 2) and in zero magnetic field (curve 1) for $C_{0.15}Mn_{0.85}S$.

The samples were subjected to X-ray diffraction analysis prior to and after the measurements of temperature dependences of the magnetic susceptibility $\chi(T)$ and the resistivity $\rho(T)$. According to the X-ray diffraction data, $Co_xMn_{1-x}S$ samples with $0 < x < 0.4$ have the NaCl-type FCC lattice structure, characteristic of α-MnS. With an increase in the degree of cation substitution (x), the lattice parameter linearly decreases from ~5.222 A ($x = 0$) to ~5.204 A ($x = 0.4$), which evidences the formation of α-MnS-based solid solutions in the system. The resistivity was measured by a standard four-probe compensation method with a dc current in the temperature range 80–300 K upon cooling the samples in zero magnetic field and in a field $H = 5$ kOe. The magnetic properties were investigated with a SQUID magnetometer in fields up to $H = 0.5$ kOe in the temperature range 4.2–300 K.

For the $Co_{0.15}Mn_{0.85}S$ composition, the magnetization M measurements in the magnetic fields $H = 13$ and 500 Oe reveal the change in the magnetization of the sample cooled in zero magnetic field and in the field $H = 13$ Oe (Fig. 1) at $T < 250$ K. With an increase in magnetic field to 500 Oe, the dependences nearly coincide. The temperature at which the irreversible change in $M(T)$ starts appearing in the magnetic properties is much higher than the Néel temperature $T_N = 175$ K.

The relative length change due to thermal expansion has been measured using a DIL-402C dilatometer (NETZSCH) in the temperature range 120–300 K in the dynamic regime. The experiments were performed on cooling and subsequently heating the sample, in both cases at a temperature rate of 5 K/min. Calibration and accounting for the thermal expansion of the measuring system were performed using fused quartz and corundum etalons.

The results of the investigation of the deformation $\Delta L/L$ and coefficient of thermal expansion $\alpha(T)$ for the two $Co_xMn_{1-x}S$ samples with $x = 0.05$ and $x = 0.15$ are presented in Fig. 2. The negative deformation change in the magnetically ordered area with an decrease in temperature points to the lattice compression. One can clearly see two $\alpha(T)$ anomalies at $T = 120$ K and below $T = 165$ K for $x = 0.05$ and at $T = 175$ K for $x = 0.15$. The coefficient of thermal expansion changes near the Néel temperature $T_N = 165$ K for $x = 0.05$ and $\alpha(T_N)/\alpha\ (T = 300) \simeq 2$ with $x = 0.15$ in the vicinity of $T_N = 175$ K in the $Co_xMn_{1-x}S$ solid solutions.

As the cobalt concentration grows, the magnetoelastic interaction strengthens. As a result, the lattice is deformed and the lattice constant increasing with increasing temperature. The temperature dependence $a(T)$ given in Fig. 3 was obtained by displacement of

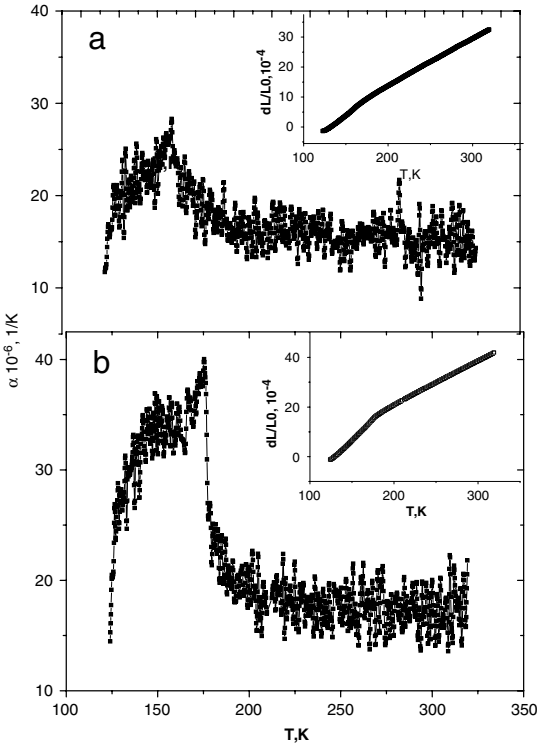

Fig. 2. Temperature dependence of the coefficient of thermal expansion for $Co_{0.05}Mn_{0.95}S$ (a) and $Co_{0.15}Mn_{0.85}S$ (b). The insets present the deformation ($\Delta L/L$) versus temperature data for $Co_{0.05}Mn_{0.95}S$ and $Co_{0.15}Mn_{0.85}S$.

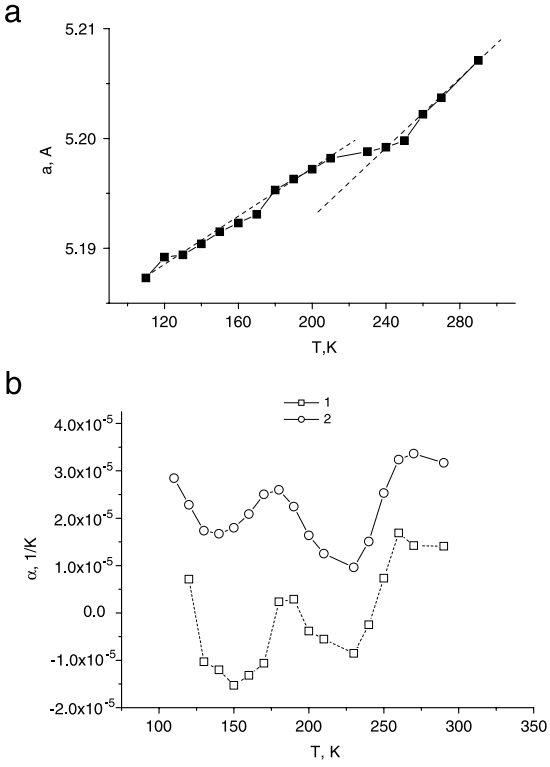

Fig. 3. Temperature dependence of the lattice constant for the $Co_{0.15}Mn_{0.85}S$ sample (a) and the coefficient of thermal expansion determined from the lattice constant $1/a da/dT$ (2) and from the difference $\alpha(T) - (da/dT)1/a$ (1) (b).

the most intensive (200) peak. No peak splitting within the measurement error $\Delta\theta = 0.03^\circ$ was found. Expansion of the lattice parameters take place and severe departures from linear dependence of $a(T)$ are revealed at $T = 120$ K, $T = 175$ K and $T = 250$ K. Weak anomalies (slope increase) are detected at the magnetic order transition temperature. A drastic slope change is observed at $T = 250$ K, which coincides with the appearance of an anomaly in the magnetic susceptibility measurements, which was associated with the orbital ordering. The absence of significant volume changes at highest temperatures indicates that the transition taking place at $T = 250$ K is really an effect related to the ordering of the electronic orbitals.

The difference in temperature behavior of the coefficient of thermal expansion $\alpha(a)$ and $\alpha(\Delta L)$ at $T < 250$ K determined by the (200) peak displacement from an X-ray diffraction pattern and by relative extension of a polycrystalline sample (Fig. 3) can be caused by two factors: lattice distortion or the occurrence of elastic stresses due to the interaction of oscillation modes with an exciton by means of the electron–phonon interaction. Generally, the lattice constant increases with temperature; however, one can separate the inhomogeneous areas related to localization of excitons and estimate their own coefficient of thermal expansion as the difference in the coefficients of thermal expansion of the sample and the lattice constant $(\mathrm{d}a/\mathrm{d}T)1/a - \alpha(T)$ (dotted line in Fig. 3(b)). The change in exciton localization radius at temperatures $T = (125–175)$ K, and $T = (185–240)$ K for the $Co_xMn_{1-x}S$ composition with $x = 0.15$ reflects on the elastic properties and, consequently, leads to modification of the elastic-strain tensor.

Conductivity electrons localized in a small microregion lead to ferromagnetic exchange as a result of s–d interaction that coexists with superexchange interactions. Thus a more likely scenario is that the large α can be attributed to the simultaneous existence of these distinctly different magnetic exchange interactions.

The resistivity measured at a fixed dc current value appears to depend on the external magnetic field. The current–voltage characteristics exhibit a weak nonlinear dependence: their slope changes with an increase in the external magnetic field in the temperature range 175 K $< T <$ 240 K (Fig. 4). With a decrease in temperature, hysteresis is observed in the current–voltage characteristic with the occurrence of the constant potential difference in the absence of current, which is typical for ferroelectrics.

These effects are caused by localization of electrons on the t_{2g} orbitals in some areas randomly distributed over the lattice. The magnetic field via the spin–orbital coupling eliminates spatial degeneracy of the autolocalized electron states and aligns the orbital moments along the magnetic field. As a result, the width of the potential barriers increases and the tunnel current decreases.

The magnetic structures of the orbital moments are characterized by the substantial anisotropy of the effective exchange interactions. For the t_{2g} orbitals, this anisotropy is caused by the spin–orbital interaction and its value is $\sim\lambda^2/E_{JT} = 8$ cm^{-1} at the spin–orbital coupling parameters $\lambda = 80$ cm^{-1} and $E_{JT} = 840$ cm^{-1}. As a result, a different population of the d_{xy}, d_{xz}, and d_{yz} orbitals is induced, and orbital ordering takes place, accompanied by ordering the orbital angular moments at the temperature $T = 230$ K.

The current carriers in the $Co_{1-x}Mn_xS$ solid solutions are charged excitons, which are pinned below the Debye temperature and form areas with an enhanced concentration of conductivity electrons and elastic deformations. The external magnetic field aligns the orbital moment and changes the direction of local deformation of the lattice, which leads to spatial anisotropy of the hopping integrals and the change in mobility of the carriers; correspondingly, the resistance grows. The competition between ordering the orbital angular moments and lattice deformation leads to the bistable state of the charge distribution and the appearance of different electric potentials at zero current.

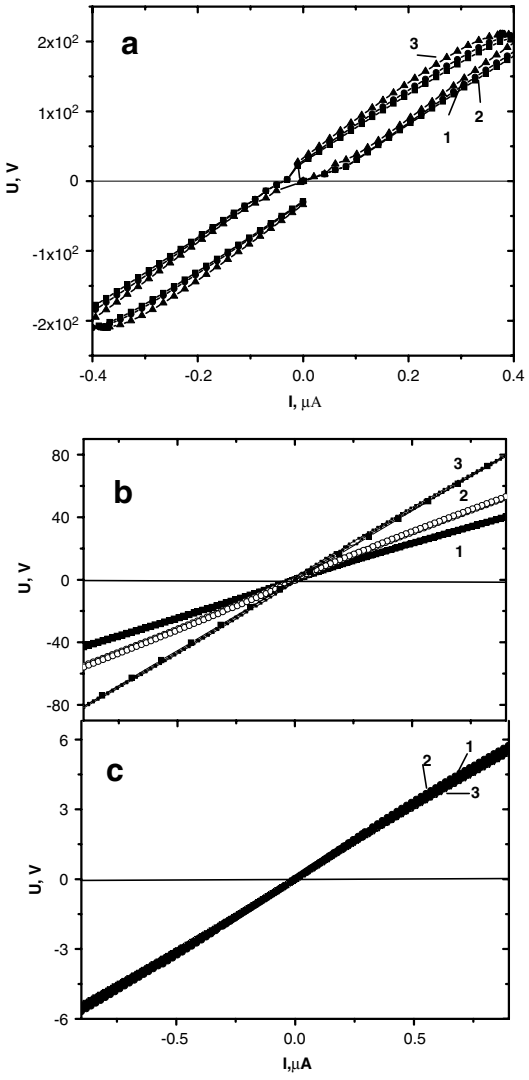

Fig. 4. Current–voltage characteristic of the $Co_{0.05}Mn_{0.95}S$ sample taken in fields of $H = 0$ kOe(1), 2 kOe(2), and 5 kOe(3) at temperatures of 176 K (a), 200 K (b), and 240 K (c).

3. Conclusions

A magnetic phase transition from the paramagnetic state to a state with long-range antiferromagnetic order has been found by the sharp drop of the coefficient of thermal expansion which points to the presence of a magnetoelastic effect. The effect of prehistory of the sample on the temperature dependence of magnetic susceptibility, resistance, and the difference between the relative changes in sample size found from the dilatometric and temperature dependences of the lattice constant are caused by the formation of an inhomogeneous structure with orbital-charge ordering.

The competition of the Coulomb interactions between the electrons located on one orbital and on different orbitals along with the change in the hopping integrals causes ordering of the electrons on certain orbitals and orbital magnetism. Due to the redistribution of the electron density, the elastic energy changes and coupled modes of the ion oscillations are induced under the action of electron–phonon interaction.

Acknowledgements

This work was supported by the Russian Foundation for Basic Research projects no. 08-02-00364-a, no. 08-02-90031, no. F08-037, F08-229, and no. 09-02-00554-a.

References

[1] K.I. Kugel, D.I. Khomskii, Sov. Phys. JETP 52 (1981) 501.
[2] Y. Tokura, N. Nagaosa, Science 288 (2000) 462.
[3] V.I. Anisimov, I.S. Elfimov, M.A. Korotin, K. Terakura, Phys. Rev. B 55 (1997) 15494.
[4] M.B. Salamon, M. Jaime, Rev. Modern Phys. 73 (2001) 583.
[5] C. Castellani, C.R. Natoli, J. Ranninnger, Phys. Rev. B 18 (1978) 4945.
[6] W. Bao, Phys. Rev. Lett. 78 (1997) 507.
[7] H. Sawada, K. Terakura, Phys. Rev. B 58 (1998) 6831.
[8] Y. Ren, et al., Nature 396 (1998) 441.
[9] C. Marquina, M. Sikora, M.R. Ibarra, A.A. Nugroho, T.T.M. Palstra, J. Magn. Magn. Mater. 290–291 (2005) 428.
[10] S. Yamaguchi, Y. Okimoto, Y. Tokura, Phys. Rev. B 54 (1997) R8666.
[11] M.A. Korotin, et al., Phys. Rev. B 54 (1996) 5309.
[12] S.S. Aplesnin, L.I. Ryabinkina, G.M. Abramova, et al., Phys. Rev. B 71 (2005) 125204.
[13] S.S. Aplesnin, L.I. Ryabinkina, O.B. Romanova, D.A. Velikanov, A.D. Balaev, D.A. Balaev, K.I. Yanushkevich, A.I. Galyas, O.F. Demidenko, O.N. Bandurina, J. Exp. Theoret. Phys. 106 (2008) 765.